Nitrogen Fixation

A Chatt-Type Catalyst with One Coordination Site for Dinitrogen Reduction to Ammonia

Tobias A. Engesser, Andrei Kindjajev, Jannik Junge, Jan Krahmer, and Felix Tuczek*[a]

Abstract: With [Mo(N_2)($P_2^{Me}PP_2^{Ph}$)] the first Chatt-type complex with one coordination site catalytically converting N_2 to ammonia is presented. Employing SmI_2 as reductant and H_2O as proton source 26 equivalents of ammonia are generated. Analogous Mo^0-N_2 complexes supported by a combination of bi- and tridentate phosphine ligands are catalytically inactive under the same conditions. These findings are interpreted by analyzing structural and spectroscopic features of the employed systems, leading to the conclusion that the catalytic activity of the title complex is due to the strong activation of N_2 and the unique topology of the pentadentate tetrapodal (pentaPod) ligand $P_2^{Me}PP_2^{Ph}$. The analogous hydrazido(2-) complex [Mo(NNH_2)($P_2^{Me}PP_2^{Ph}$)](BAr^F)$_2$ is generated by protonation with $HBAr^F$ in ether and characterized by NMR and vibrational spectroscopy. Importantly, it is shown to be catalytically active as well. Along with the fact that the structure of the title complex precludes dimerization this demonstrates that the corresponding catalytic cycle follows a mononuclear pathway. The implications of a PCET mechanism on this reactive scheme are considered.

The activation of molecular nitrogen has been of great interest over the last decades. This in particular refers to biological nitrogen fixation, which is mediated by the enzyme nitrogenase. Although the structure of this enzyme has been fully determined,[1] the mechanism of the dinitrogen reduction and protonation is still the subject of current research.[2] To mimic this process and elucidate its mechanism, various small-molecule based model systems have been studied in detail.[3] The earliest of these systems were established by Chatt and Hidai on the basis of molybdenum (bis)dinitrogen complexes with phosphine coligands.[4] In 1985 Pickett et al. demonstrated an electrochemical synthesis of NH_3 mediated by a tungsten complex.[5] The first truly catalytic reduction of N_2 to ammonia was achieved by Schrock et al. in 2003 using a triamidoamine molybdenum complex (Scheme 1) as catalyst, Cp^*_2Cr as reductant and LutH(BAr^F) as proton source. This system generated 7.6 equivalents of NH_3,[6] which clearly was a milestone in synthetic nitrogen fixation. A N_2-bridged dinuclear Mo system supported by pincer ligands, presented by Nishibayashi et al. in 2011, led to 23.2[7] (through modification up to several hundred)[8,9] equivalents of ammonia. While this group first employed LutH(OTf) as acid and Cp^*_2Cr as reductant, an even more powerful protocol was established in 2019, involving SmI_2/H_2O as reductant and proton source. This way, 4.350 equivalents of ammonia could be generated.[10] In 2013, the first non-molybdenum catalytic system for N_2 reduction was presented by Peters et al., employing a BP_3-supported iron complex, KC_8 as reductant and $HBAr^F$ as acid.[11]

On the basis of the classic Chatt-type bis(dinitrogen) Mo/W complexes containing diphosphine coligands (e.g., dppe or depe) the first mechanism for the transition-metal mediated conversion of N_2 to NH_3 was formulated, the so-called *Chatt cycle* (Scheme 2).[12]

This reactive scheme starts with the protonation of the parent N_2 complex, leading to the hydrazido(2-) complex. In the subsequent steps, one additional proton and two electrons are required to cleave the N–N bond and generate the first equivalent of ammonia.[13,14] This mechanism is very similar (but not identical) to the *Schrock cycle*, which is based on the

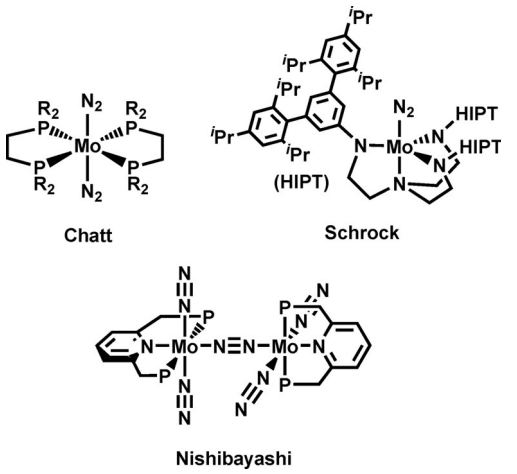

Scheme 1. Molybdenum-based model systems for synthetic nitrogen fixation.[4,6]

[a] Dr. T. A. Engesser, A. Kindjajev, J. Junge, Dr. J. Krahmer, Prof. Dr. F. Tuczek
Institut für Anorganische Chemie
Christian-Albrechts-Universität zu Kiel
Otto-Hahn-Platz 10, 24118 Kiel (Germany)
E-mail: ftuczek@ac.uni-kiel.de

Supporting information and the ORCID identification number(s) for the author(s) of this article can be found under:
https://doi.org/10.1002/chem.202003549.

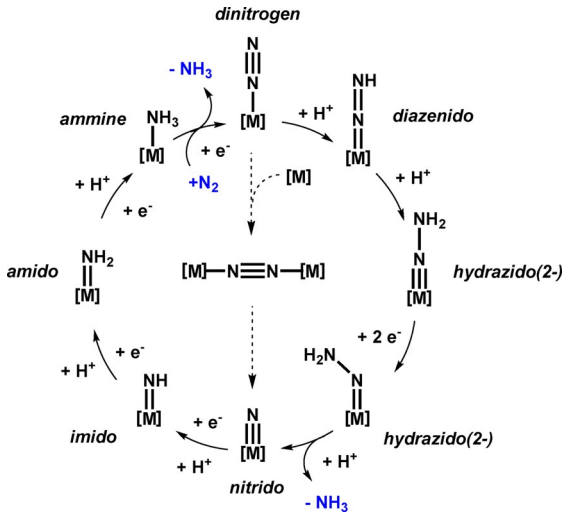

Scheme 2. Chatt cycle (solid arrows); dotted: dinuclear pathway with N–N cleavage.

Mo triamidoamine complex.[15,16] In this context it should be noted that both the *Chatt*- and the *Schrock cycle* involve N–N splitting at the level of NNH_2- and NNH_3-complexes, whereas the dinuclear systems of Nishibayashi et al. (Scheme 1) mediate N–N cleavage of the parent N_2-complexes, leading to two nitrido intermediates, which subsequently are converted to NH_3.[7,9] Recently, this scenario has also been evidenced in a classic Chatt system by Masuda and co-workers, where the dinuclear Mo^{I} complex $[\{Mo(depe)_2\}_2(\mu\text{-}N_2)]^{2+}$ was found to split into two $[Mo(N)(depe)_2]^{+}$ cations by cleavage of the N–N bond (Scheme 3).[17] Similar reactivities have been obtained with other dinuclear, dinitrogen-bridged transition metal) complexes.[9,18]

An important disadvantage of the original Chatt systems has been the fact that protonation of the dinitrogen complex involves exchange of one of the two N_2 ligands by the conjugate base of the applied acid, causing a 50% loss of bound substrate. Moreover, this anionic *trans*-coligand had to be exchanged again at the end of the cycle leading to the bis(dinitrogen) complex, and Mo^{I} complexes formed as intermediates during that stage were found to be prone to disproportionation.[14,19] These mechanistic drawbacks have traditionally been invoked to rationalize that classic Chatt-type systems, although in principle forming all relevant intermediates, are catalytically inactive towards the conversion of N_2 to NH_3. On the other hand, Nishibayashi et al. recently showed that Chatt complexes

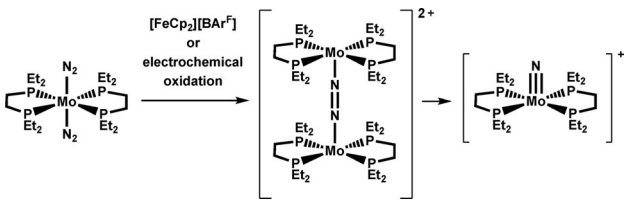

Scheme 3. Formation of a dinuclear Mo^{I} complex from $[Mo(N_2)_2(depe)_2]$ via one-electron oxidation, leading to a Mo^{IV} nitrido complex by dinitrogen cleavage; adapted from Masuda et al.[17]

with mono- and bidentate ligands indeed catalyse the generation of ammonia from N_2 if SmI_2/H_2O (or SmI_2/alcohol) is used as reductant and proton source.[20] Using *cis*,*mer*-$[Mo(NNH_2)(OTf)_2(PMePh_2)_3]$ as example for a NNH_2 intermediate also led to catalytic amounts of NH_3. From this observation it was inferred that the SmI_2-mediated reduction pathway of Chatt-type complexes probably follows the Chatt cycle.

In view of the above-mentioned problems of the classic Chatt complexes, we had in the past developed a series of molybdenum dinitrogen complexes in which the *trans* position is occupied by a donor atom of a multidentate ligand. These systems were intended to provide only one site for the coordination and reduction of N_2 and avoid all other ligand exchange reactions occurring at the single Mo center. Initially, we had employed a combination of a tripodal (**1**)[21] or a linear tridentate ligand (**2**)[22] with a bidentate co-ligand (Scheme 4) for this purpose. Compounds **2** and **1**, however, suffered from isomerization and, respectively, instability of the tridentate phosphine ligand coordination upon protonation of the N_2-complex, which was ascribed to the fact that the *trans*-donor is not fixed strongly enough to the center Mo atom. Later we succeeded combining the two described approaches into a unique pentadentate tetrapodal (**pentaPod**) phosphine ligand. Based on this concept, the molybdenum mono(dinitrogen) complex $[Mo(N_2)(P_2^{Me}PP_2^{Ph})]$ (**3**) was synthesized and characterized both experimentally and theoretically.[23]

We now discovered that reaction of **3** in THF with N_2 gas at 1 atm, 180 equiv of SmI_2 and 180 equiv of H_2O gives 25.73 ± 0.37 equiv of ammonia based on the molybdenum atom (43% yield based on SmI_2; Table 1). Replacing $^{14}N_2$ by $^{15}N_2$ in these experiments correspondingly leads to $^{15}NH_3$ which was detected by ^{1}H-NMR as $^{15}NH_4Cl$ (cf. SI, Figure S1). To check if the pentadentate coordination of **3** is responsible for the catalytic activity, complexes **1** and **2** with tridentate or tripodal ligands were investigated under the same conditions. However, both only led to substoichiometric amounts (less than 2 equiv) of ammonia, which indicates decomposition of the complexes. In order to understand the different catalytic activities of **1**, **2** and **3**, the electronic and geometric structures of these systems are analysed in the following.

The key property of a molecular catalyst for synthetic nitrogen fixation is the activation of the N_2 ligand,[24] enabling its protonation and further reduction to ammonia. The most sensitive probe of this capability is the N–N stretching frequency. In this respect, complex **3** exhibits the highest activation (Table 1). As a matter of fact, its N–N stretching frequency is the lowest of all known Mo-pentaphosphine complexes. In comparison, ν_{NN} of **1** and **2** are by 45 and 50 cm^{-1} higher, re-

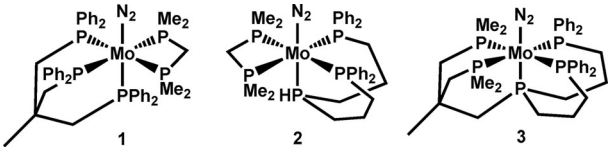

Scheme 4. $[Mo(N_2)(tdppme)(dmpm)]$ (**1**)[21] $[Mo(N_2)(prPPHP)(dmpm)]$[22] (**2**), and $[Mo(N_2)(P_2^{Me}PP_2^{Ph})]$ (**3**).[23]

Table 1. Experimental and calculated spectroscopic and structural parameters of the employed molybdenum pentaphosphine complexes and ammonia formation in the presence of them.

Catalyst	NH_3 production[a]	NN stretch [cm^{-1}]	d(Mo-P_{ax}) [pm]	d(Mo-N) [pm]	d(N-N) [pm]	d(Mo-P_{eq}) av. [pm]	$^2J(^{31}P_M, ^{15}N_\alpha)$ [Hz]	$^3J(^{31}P_M, ^{15}N_\beta)$ [Hz]
[Mo(N_2)(tdppme)(dmpm)] (**1**)	0.82 ± 0.04	1979	244.54(16)	206.6(6)	106.9(8)	246.21	–	–
[Mo(N_2)(prPPHP)(dmpm)] (**2**)	1.77 ± 0.03	1974	240.15(6)	202.1(2)	111.6(3)	242.96	14.1	1.2
[Mo(N_2)($P_2^{Me}PP_2^{Ph}$)] (**3**)	25.73 ± 0.37	1929	238.68(12)	203.3(5)	109.9(5)	244.81	13.5	1.4
[Mo(NNH_2)($P_2^{Me}PP_2^{Ph}$)]$^{2+}$ (**4**)	26.14 ± 0.32	1490[b]	261.17[b]	177.4[b]	131.7[b]	252.51[b]	23.2	7.6

[a] equivalents per Mo atom; N_2 gas at 1 atm, 180 equiv of SmI_2 and 180 equiv of H_2O; [b] PBE0-D3(BJ)/def2-SVP.

spectively. The activation of N_2 is a function of the electron density on the Mo^0 center, which in turn sensitively depends on the type of phosphine donors. Note that all three complexes have an equatorial P_{eq} coordination of two PMe_2 and two PPh_2 groups, whereas the nature of the phosphine in *trans*-position is different. In a first approximation, the activation of N_2 in complexes **1**–**3** thus is a function of the axial phosphine donor P_{ax}, and in view of the fact that electron donation increases within the sequence $PPh_3 < PR_2H < PR_3$ (R = alkyl),[25] the observed sequence of ν_{NN} can qualitatively be understood.

Besides these electronic factors, it is also of interest to analyze the Mo–N and Mo–P_{ax} distances in **1**–**3**. Importantly, **3** has the shortest Mo–P_{ax} bond of all complexes, also being shorter than all Mo–P_{eq} bonds (Table 1). The Mo–P_{ax} distance of **2** is slightly longer, whereas that of **1** is much longer, getting similar to the Mo-P_{eq} values (≈2.4 Å). The short Mo–P_{ax} distances of **3** and **2** indicate strong Mo–P_{ax} bonds, which serves to transfer electron density to the Mo^0 center. Remarkably, the Mo–N bonds are short in these complexes as well. This should lead to strong P_{ax}-Mo-(N_2) interactions which may be probed by ^{31}P- and ^{15}N-NMR spectroscopy.

The ^{31}P NMR spectrum of **3** shows an AA'MXX' pattern, in agreement with its pentaphosphine environment (Figure 1 a). In order to obtain information regarding the coupling between the phosphine ligands and the N atoms of the coordinated N_2, the isotopically labeled complex was synthesized. Additional couplings between the P donors and the N_α and N_β atoms of the dinitrogen ligand are visible in the ^{31}P-NMR spectrum of **^{15}N-3** (Figure 1 b and c). The M signal, which belongs to P_{ax} (Figure 1 d), exhibits much stronger couplings ($^2J(^{31}P_M, ^{15}N_\alpha)$ = 13.5 Hz, $^3J(^{31}P_M, ^{15}N_\beta)$ = 1.4 Hz) than the phosphine groups P_{eq} in *cis*-position ($^2J(^{31}P_A, ^{15}N_\alpha)$ = 3.1 Hz, $^3J(^{31}P_A, ^{15}N_\beta)$ < 1.0 Hz; $^2J(^{31}P_X, ^{15}N_\alpha)$ = 3.0 Hz, $^3J(^{31}P_X, ^{15}N_\beta)$ = 1.0 Hz; cf. SI, Figures S2, S3).

In the M part of the spectrum, an asymmetric positioning of the ^{15}N (dd-) signal with regard to the ^{14}N signal deriving from residual **3** is noticed (Figure 1 d), which corresponds to a two-bond (tertiary) ^{15}N-induced isotope effect on the chemical shift of the *trans* ^{31}P nucleus ($^2\Delta^{31}P(^{15}N)$). We ascribe this phenomenon to the anharmonicity of the Mo-(N_2) potential, leading to a slight reduction of the Mo–N_α equilibrium bond distance if the mass of the N_2 ligand is increased. This in turn increases the Mo–P_{ax} bond length by virtue of the *trans* effect, causing an increased shielding of P_{ax}. With an upfield shift of around 1 Hz (6.2 ppb) the two-bond isotope shift across the metal center is in a range where usually one-bond $^{14}N \rightarrow ^{15}N$ shifts (e.g., phosphoric acid amide: 9.6 ppb[26]) are observed. This indeed reflects a strong influence of the N_2 coordination on the bonding of the P-atom in *trans* position.

In order to elucidate a possible dependence of this effect on the electronic structure of the Mo-(N_2) complex, the ^{31}P-NMR spectra of complex **2**, which also exhibits a short Mo–P_{ax} bond (cf. Table 1), were re-examined (cf. SI, Figures S4–S6). This analysis provided similar results ($^2\Delta^{31}P(^{15}N)$ = 1.1 Hz (6.9 ppb). Moreover, the $J(^{31}P_M, ^{15}N)$ coupling constants were determined to 14.1 (N_α) and 1.2 Hz ($^{15}N_\beta$), respectively, quite close to the values of **3** (Table 1). In case of complex **1** having the longest Mo–P_{ax} bond of all three complexes, an analogous analysis was not possible due to its ^{31}P-NMR spectrum being of higher order (cf. SI, Figure S7). As the bonding situation drastically changes along the *Chatt cycle*, it also appeared of interest to explore a possible correlation between $^2\Delta^{31}P(^{15}N)$ and the electronic structure of the respective intermediates.

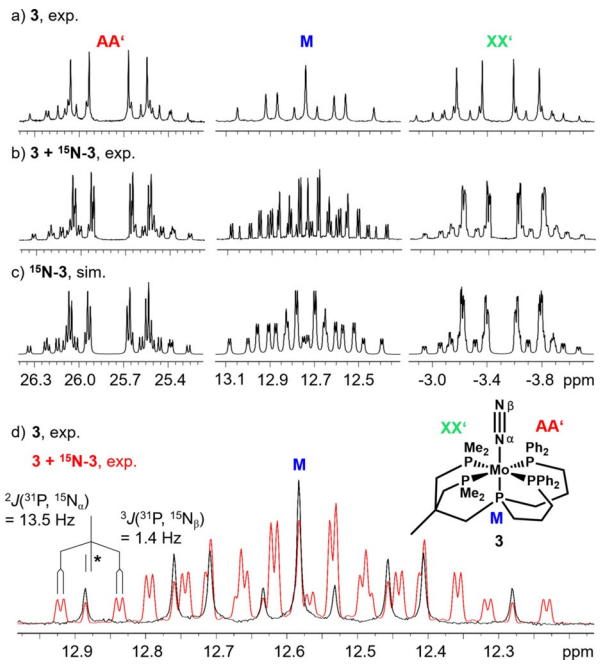

Figure 1. a) Experimental (in C_6D_6) ^{31}P-NMR spectra of **3** and b) a mixture of **3** and **^{15}N-3** (18% **3**). c) Simulated spectrum of **^{15}N-3**. d) Overlay of experimental M signals of **^{14}N-3** and the mixture, showing the two-bond (tertiary) ^{15}N-induced isotope effect (* $^2\Delta\delta$ = 1.0 Hz, 6.2 ppb).

Protonation of **3** with $[H(OEt_2)_2][BAr^F]$[27] in Et_2O ("$HBAr^F$") affords the NNH_2 complex $[Mo(NNH_2)(P_2^{Me}PP_2^{Ph})][BAr^F]_2$ (**4**). This is, for example, evident from the vibrational spectra of solid **4** (**^{15}N-4**) showing N–H (^{15}N–H) stretches at 3312 (3307) cm^{-1} (ν_{as}(NH)) and 3200 (3198) cm^{-1} (ν_s(NH)) as well as the disappearance of ν_{NN} at 1929 cm^{-1} (cf. SI, Figure S8 and Table S1; preliminary spectroscopic data of **4** were already given in ref. [23]). In analogy to **3**, the ^{31}P-NMR spectrum of **4** exhibits an AA'MXX' pattern, with chemical shifts and coupling constants modified with respect to the former (Figure 2 a; cf. SI, Figure S9–S13). This indicates that the **pentaPod** environment of **3** is retained upon protonation, a prerequisite for the catalytic activity of our system. Protonation was also performed with **3** containing a mixture of $^{14}N_2$ and $^{15}N_2$ (18% ^{14}N; see above). Again, the resulting ^{31}P-NMR spectrum (Figure 2 b) shows a superposition of the spectra mainly deriving from the $^{15}N^{15}NH_2$ complex (Figure 2 c) with small additional signals from the $^{14}N^{14}NH_2$ isotopomer. In contrast to the parent N_2 complex **3**, however, no ^{15}N-isotope effect on the ^{31}P-NMR shift is visible in the M-part of **4**/**^{15}N-4** (Figure 2 d).

In order to interpret this result, we note that DFT predicts a hydrazido(2-) configuration for **4** (cf. SI, Figure S14), with a triple bond between Mo and N_α.[28] This is in contrast to classic Chatt-type NNH_2 complexes such as $[MoF(NNH_2)(diphos)_2]$ where an isodiazene description was found to be more appropriate.[29] The lack of $^2\Delta^{31}P(^{15}N)$ on $\delta(P_M)$ suggests that the anharmonicity in the Mo≡N potential of **4** is much lower than in the Mo-N_2 bond of the parent dinitrogen complex **3**. The triply bonded NNH_2 ligand should exert a strong *trans* effect. This is supported by DFT calculations which indicate a significant elongation of the Mo–P_{ax} distance in **4** with respect to **3**, making it even longer than the Mo–P_{eq} bonds (Table 1). Correspondingly, the protonation-induced high-field shift is much larger for the M signal than for the A and X signals (cf. SI, Figure S13 and Table S2).

The flexibility of the metal–E bond in *trans*-position to the nitrogenic ligand has been considered by Peters et al. as an important criterion for the catalytic activity of their iron-dinitrogen complexes supported by EP_3 ligands (E = B, Si, C).[30] In spite of the short Mo–P_{ax} bond observed for the Mo-dinitrogen complex **3** it appears that the **pentaPod** ligand framework is sufficiently flexible to allow elongation of the axial Mo–P bond in the NNH_2-complex **4**.[28]

Formation of the hydrazido(2-) complex **4** is also evident from its ^{1}H-^{15}N-HMBC spectrum which clearly shows the -NNH_2 moiety; i.e., a doublet in the ^{1}H dimension with a $^1J(^{15}N_\beta, ^1H)$ of 94.6 Hz and a corresponding triplet in the ^{15}N spectrum (Figure 3; cf. SI for complete spectrum, Figure S15). In the ^{15}N spectrum the couplings of N_β to N_α (11.2 Hz) and the *trans* standing P_M (7.6 Hz) are also observable (cf. SI, Figure S16, Tables S3 and S4).

In analogy to **3**, compound **4** was applied as a catalyst for the reduction of N_2 at 1 atm with 180 equiv of SmI_2 and 180 equiv of H_2O in THF. As the stability of **4** in this solvent had been found to be limited,[23] we generated **4** in situ in diethyl ether and subsequently added this to a solution of SmI_2/H_2O in THF. These experiments afforded 26.14 ± 0.32 equiv of NH_3 (Table 1), identical to the yield obtained with the N_2 complex **3** within the error limit. This proves the role of the hydrazido(2-) complex **4** as an intermediate in the catalytic conversion of N_2 to NH_3 mediated by **3** and suggests that the corresponding mechanism follows the Chatt cycle; e.g., avoids a direct N≡N cleavage (Scheme 2). Furthermore, the fact that dimerization of **3** is sterically hindered renders the existence of a dinuclear pathway (Scheme 3) improbable. A simulation of a corresponding Mo^I or Mo^0 dimer leads to dissociation of one Mo–P bond (SI, Figure S17).

The usual formulation of the Chatt cycle starts with two protonations of the Mo^0-N_2 complex, leading to the NNH_2 complex (cf. Scheme 2); notably, **4** has been generated from **3** this way. On the other hand, the SmI_2/water complex is known to react with protonatable/reducible substrates by proton-coupled electron transfer (PCET).[31] In this context, it has become customary to assess the N_2-reducing capacity of a catalytic nitro-

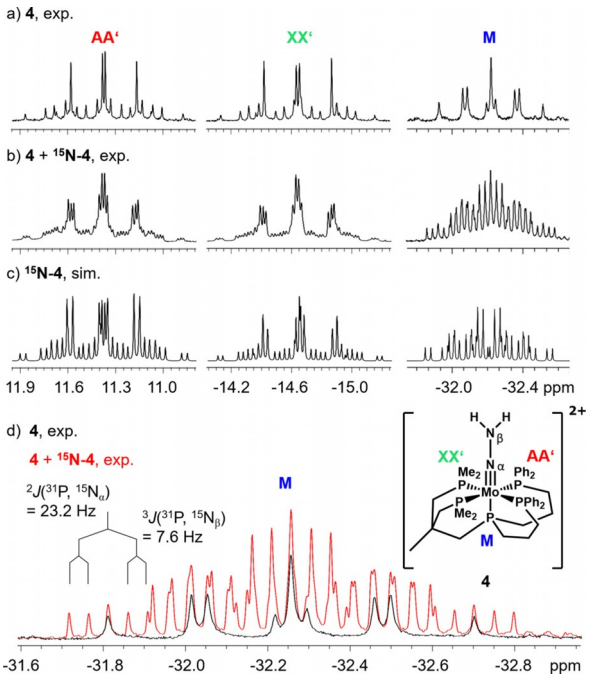

Figure 2. a) Experimental (in d10-Et_2O) ^{31}P-NMR spectra of **4** and b) a mixture of **4** and **^{15}N-4** (18% **4**). c) Simulated spectrum of **^{15}N-4**. d) Overlay of experimental M signals of **^{14}N-4** and the mixture.

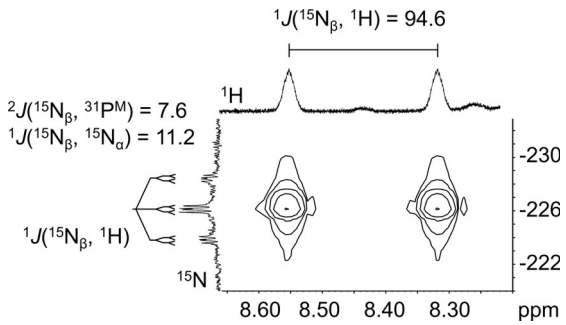

Figure 3. Enlarged $N_\beta H_2$ part of the ^{1}H-^{15}N-HMBC spectrum of **^{15}N-4** in *d10*-Et_2O.

genase model system by quoting the N–H bond dissociation free energy (BDFE) of the respective NNH (diazenido) complex (cf. Scheme 2). In order to exergonically transfer one electron and one proton to the N_2 complex, the BDFE of the former has to exceed that of the employed PCET reagent or the effective BDFE of the employed acid/reductant combination, respectively.[32]

To determine the N–H BDFE of the NNH-intermediate for a given N_2-reduction catalyst, DFT calculations may be employed.[20] Transfer of one electron and one proton to the Mo^0-dinitrogen complex leads to the neutral Mo^I-diazenido(−) intermediate. An estimate of the corresponding energetics was obtained by DFT, simulating the reaction of [Mo(N_2)(pentaPod)] with TEMPO-H, a H-atom transfer reagent having a well-defined O–H BDFE of 65.2 kcal mol^{-1} in benzene,[33] to give the [Mo(NNH)(pentaPod)] complex. Subtraction of the reaction TEMPO-H → TEMPO$^{\bullet}$ + H$^{\bullet}$ leads to a N–H BDFE of 19.2 kcal mol^{-1} for the Mo^I-diazenido(−) complex ($\Delta_{r,theo}G^{298}$(solv, benzene), cf. SI, Table S6), which is somewhat lower than the O–H BDFE of SmI_2/water (26 kcal mol^{-1}).[31] PCET from this reagent to the $Mo^0(N_2)$ complex thus is slightly endergonic ($\Delta G^{298} = +6.8$ kcal mol^{-1}), but thermodynamically feasible.

In view of the fact that the diazenido(−) intermediates of the classic Chatt cycle correspond to Mo^{II} (and not Mo^I) species,[29] we also theoretically investigated the formation of $[Mo^{II}(NNH)(pentaPod)]^+$ by PCET from the corresponding cationic $Mo^I(N_2)$-complex. An analogous procedure as described above gives a N–H BDFE of 52.5 kcal mol^{-1} for the Mo^{II}-diazenido(−) intermediate ($\Delta_{r,theo}G^{298}$(solv, benzene), cf. SI, Table S6). This value well exceeds the BDFE of SmI_2/water (see above), rendering PCET to the cationic $[Mo^I(N_2)(pentaPod)]^+$ complex highly exergonic ($\Delta G^{298} = -26.5$ kcal mol^{-1}). On the other hand, neutral [$Mo^0(N_2)$(pentaPod)] (**3**) was successfully employed as catalyst in our SmI_2/water-mediated N_2-to-NH_3 conversion experiments (see above). In the framework of a PCET mechanism it thus remains to be elucidated whether (and, if yes, how) our system switches from a pathway starting from a $Mo^0(N_2)$ complex to an energetically more favourable reaction path that involves a mononuclear, cationic $Mo^I(N_2)$ intermediate.

In summary, three structurally related Mo-N_2 complexes with pentaphosphine environment have been investigated as catalysts for the conversion of N_2 to NH_3, using SmI_2/H_2O as protonating agent and reductant. Only the title complex [Mo(N_2)($P_2^{Me}PP_2^{Ph}$)] (**3**) was found to be catalytically active. This is attributed to the fact that it exhibits the highest activation of N_2 and the **pentaPod** coordination. The strong chelate effect of this ligand creates an inert and stable, yet flexible ligand environment allowing protonation and reduction of the Mo^0-N_2 complex under retention of the pentaphosphine ligation. Protonation of the dinitrogen complex **3** leads to the hydrazido(2-) complex **4** which was isolated and spectroscopically characterized. Importantly, **4** was also found to be catalytically active. Along with the fact that the Mo(N_2)-**pentaPod** complex precludes dimerization this demonstrates the existence of a mononuclear pathway along the Chatt cycle for the N_2-to-NH_3 conversion catalyzed by this system. The implications of a PCET mechanism on this pathway are considered.

Acknowledgements

The authors thank the spectroscopic department, especially S. Pehlke and J. Pick for measurements, B. M. Flöser for help and fruitful discussions concerning the calculations and S. Froitzheim for designing the cover, as well as CAU Kiel for financial support of this research. Open access funding enabled and organized by Projekt DEAL.

Conflict of interest

The authors declare no conflict of interest.

Keywords: ammonia · catalysis · molybdenum · nitrogen fixation · phosphines

[1] T. Spatzal, M. Aksoyoglu, L. Zhang, S. L. A. Andrade, E. Schleicher, S. Weber, D. C. Rees, O. Einsle, *Science* **2011**, *334*, 940.
[2] a) L. C. Seefeldt, B. M. Hoffman, J. W. Peters, S. Raugei, D. N. Beratan, E. Antony, D. R. Dean, *Acc. Chem. Res.* **2018**, *51*, 2179; b) B. M. Hoffman, D. Lukoyanov, Z.-Y. Yang, D. R. Dean, L. C. Seefeldt, *Chem. Rev.* **2014**, *114*, 4041.
[3] a) N. Stucke, B. M. Flöser, T. Weyrich, F. Tuczek, *Eur. J. Inorg. Chem.* **2018**, 1337; b) Y. Nishibayashi, *Inorg. Chem.* **2015**, *54*, 9234; c) J. Chatt, J. R. Dilworth, R. L. Richards, *Chem. Rev.* **1978**, *78*, 589.
[4] J. Chatt, A. J. Pearman, R. L. Richards, *Nature* **1975**, *253*, 39.
[5] C. J. Pickett, J. Talarmin, *Nature* **1985**, *317*, 652–653.
[6] D. V. Yandulov, R. R. Schrock, *Science* **2003**, *301*, 76.
[7] K. Arashiba, Y. Miyake, Y. Nishibayashi, *Nat. Chem.* **2011**, *3*, 120.
[8] A. Eizawa, K. Arashiba, H. Tanaka, S. Kuriyama, Y. Matsuo, K. Nakajima, K. Yoshizawa, Y. Nishibayashi, *Nat. Commun.* **2017**, *8*, 14874.
[9] K. Arashiba, A. Eizawa, H. Tanaka, K. Nakajima, K. Yoshizawa, Y. Nishibayashi, *BCSJ* **2017**, *90*, 1111.
[10] Y. Ashida, K. Arashiba, K. Nakajima, Y. Nishibayashi, *Nature* **2019**, *568*, 536.
[11] J. S. Anderson, J. Rittle, J. C. Peters, *Nature* **2013**, *501*, 84.
[12] a) F. Tuczek, K. H. Horn, N. Lehnert, *Coord. Chem. Rev.* **2003**, *245*, 107; b) C. J. Pickett, *J. Biol. Inorg. Chem.* **1996**, *1*, 601; c) J. Chatt, R. L. Richards, *J. Organomet. Chem.* **1982**, *239*, 65.
[13] a) K. H. Horn, N. Böres, N. Lehnert, K. Mersmann, C. Näther, G. Peters, F. Tuczek, *Inorg. Chem.* **2005**, *44*, 3016; b) K. Mersmann, K. H. Horn, N. Böres, N. Lehnert, F. Studt, F. Paulat, G. Peters, I. Ivanovic-Burmazovic, R. van Eldik, F. Tuczek, *Inorg. Chem.* **2005**, *44*, 3031.
[14] Y. Alias, S. K. Ibrahim, M. A. Queiros, A. Fonseca, J. Talarmin, F. Volant, C. J. Pickett, *J. Chem. Soc. Dalton Trans.* **1997**, 4807.
[15] a) R. R. Schrock, *Angew. Chem. Int. Ed.* **2008**, *47*, 5512; *Angew. Chem.* **2008**, *120*, 5594; b) D. V. Yandulov, R. R. Schrock, *Inorg. Chem.* **2005**, *44*, 5542.
[16] a) W. Thimm, C. Gradert, H. Broda, F. Wennmohs, F. Neese, F. Tuczek, *Inorg. Chem.* **2015**, *54*, 9248; b) F. Studt, F. Tuczek, *Angew. Chem. Int. Ed.* **2005**, *44*, 5639; *Angew. Chem.* **2005**, *117*, 5783.
[17] A. Katayama, T. Ohta, Y. Wasada-Tsutsui, T. Inomata, T. Ozawa, T. Ogura, H. Masuda, *Angew. Chem. Int. Ed.* **2019**, *58*, 11279; *Angew. Chem.* **2019**, *131*, 11401.
[18] a) I. Klopsch, E. Y. Yuzik-Klimova, S. Schneider, *Top. Organomet. Chem.* **2017**, *60*, 71; b) G. A. Silantyev, M. Förster, B. Schluschaß, J. Abbenseth, C. Würtele, C. Volkmann, M. C. Holthausen, S. Schneider, *Angew. Chem. Int. Ed.* **2017**, *56*, 5872; *Angew. Chem.* **2017**, *129*, 5966; c) Q. Liao, A. Caviallé, N. Saffon-Merceron, N. Mézailles, *Angew. Chem. Int. Ed.* **2016**, *55*, 11212; *Angew. Chem.* **2016**, *128*, 11378; d) T. J. Hebden, R. R. Schrock, M. K. Takase, P. Müller, *Chem. Commun.* **2012**, *48*, 1851.
[19] K. Mersmann, A. Hauser, N. Lehnert, F. Tuczek, *Inorg. Chem.* **2006**, *45*, 5044.
[20] Y. Ashida, K. Arashiba, H. Tanaka, A. Egi, K. Nakajima, K. Yoshizawa, Y. Nishibayashi, *Inorg. Chem.* **2019**, *58*, 8927.

[21] J. Krahmer, H. Broda, C. Näther, G. Peters, W. Thimm, F. Tuczek, *Eur. J. Inorg. Chem.* **2011**, 4377.
[22] S. Hinrichsen, A.-C. Schnoor, K. Grund, B. Flöser, A. Schlimm, C. Näther, J. Krahmer, F. Tuczek, *Dalton Trans.* **2016**, *45*, 14801.
[23] S. Hinrichsen, A. Kindjajev, S. Adomeit, J. Krahmer, C. Näther, F. Tuczek, *Inorg. Chem.* **2016**, *55*, 8712.
[24] F. Studt, F. Tuczek, *J. Comput. Chem.* **2006**, *27*, 1278.
[25] C. A. Tolman, *Chem. Rev.* **1977**, *77*, 313.
[26] W. Gombler, R. W. Kinas, W. J. Stec, *Z. Naturforsch. B* **1983**, *38*, 815.
[27] M. Brookhart, B. Grant, A. F. Volpe, *Organometallics* **1992**, *11*, 3920.
[28] B. M. Flöser, F. Tuczek, *Coord. Chem. Rev.* **2017**, *345*, 263.
[29] a) N. Lehnert, F. Tuczek, *Inorg. Chem.* **1999**, *38*, 1659; b) N. Lehnert, F. Tuczek, *Inorg. Chem.* **1999**, *38*, 1671.
[30] S. E. Creutz, J. C. Peters, *J. Am. Chem. Soc.* **2014**, *136*, 1105.
[31] S. S. Kolmar, J. M. Mayer, *J. Am. Chem. Soc.* **2017**, *139*, 10687.
[32] M. J. Chalkley, J. Peters, *Eur. J. Inorg. Chem.* **2020**, 1353.
[33] J. J. Warren, T. A. Tronic, J. M. Mayer, *Chem. Rev.* **2010**, *110*, 6961.

Manuscript received: July 30, 2020
Revised manuscript received: August 18, 2020
Accepted manuscript online: August 20, 2020
Version of record online: October 19, 2020